AUT Journal of Mechanical Engineering

AUT J. Mech. Eng., 9(4) (2025) 403-412
DOI: 10.22060/ajme.2025.23879.6163

Presenting of a novel high-order sliding mode control based on Lyapunov theory

Masoud Abdolmohammadi, Habib Ahmadi *

Faculty of Mechanical Engineering, Shahrood University of Technology, Shahrood, Iran

ABSTRACT: In this paper, we present a novel control scheme based on high-order sliding mode control (HOSM) for nonlinear systems under uncertainty. The stability and robustness of the proposed controller have been proven using Lyapunov's method. The controller not only withstands uncertainties and disturbances but also significantly reduces the amplitude and frequency of chattering compared to existing algorithms. Furthermore, the suggested high-order sliding mode controller provides the ability to adjust the chattering frequency through its parameters. Initially, the sliding surface is introduced for second-order dynamics, followed by the necessary stability assumptions to ensure system stability. Then, a new second-order sliding mode controller is proposed, and its stability is verified through Lyapunov's method. Detailed simulation results using a planar robot demonstrate the controller's performance, which is compared with existing algorithms. The results confirm that the new controller effectively manages uncertainties, ensuring stable system control. The proposed controller not only reduced the frequency of chattering but also decreased the steady-state error for a two-link robot. Simulation shows the decrease in root mean square error compared to twisting and super-twisting controllers.

Review History:

Received: Feb. 01, 2025
Revised: May, 11, 2025
Accepted: May, 26, 2025
Available Online: Jun. 10, 2025

Keywords:

High-order Sliding Mode
Lyapunov Theory
Robust Control
Twisting Algorithm
Super Twisting Algorithm

1- Introduction

Robust nonlinear control strategies have been extensively applied to complex systems, particularly those involving significant uncertainties. Among these methods, sliding mode control (SMC) is one of the most prominent techniques due to its ability to handle uncertainties through switching control laws. By designing an appropriate sliding surface and ensuring that the system converges to and remains on this surface, SMC effectively mitigates the impact of uncertainties [1, 2].

The concept of variable structure systems (VSS) with sliding modes, for the first time, was introduced in the early 20th century and gained significant attention in control applications after Utkin's work in 1977 [1]. Since then, SMC has been widely adopted in various fields, particularly in robotic systems [3, 4]. Despite its robustness, conventional SMC suffers from a key limitation: chattering. This high-frequency oscillation can cause mechanical wear in physical systems and instability in electrical systems, thus limiting its practical applications.

Several approaches have been proposed to address the chattering phenomenon, including the development of high-order sliding mode (HOSM) controllers [5, 6]. These methods aim to reduce or eliminate chattering while maintaining robustness against uncertainties. Emel'yanov et al. (1986) introduced the use of higher-order derivatives of sliding variables, which led to the development of second-order sliding mode algorithms such as the Twisting Algorithm (TA) and Super-Twisting Algorithm (STA) [7]. These algorithms provide smoother control inputs and enhance tracking performance, particularly in systems with disturbances and unmodeled dynamics.

Further advancements in the SMC field have expanded the applicability of HOSM methods. For example, Bailey et al. introduced an SMC method for a 2-degree-of-freedom (DOF) robot in 1987, demonstrating its effectiveness in reducing the interaction between robot links [3]. In 1989, Yeung et al. utilized SMC for a flexible robot, achieving significant improvements in control accuracy [8]. The introduction of bound estimation for parametric uncertainties in 1993 further improved the performance of SMC by enabling more precise tuning of control coefficients [9]. Tzafestas et al. (1996) applied SMC to a 5-link bipedal robot, which achieved notable improvement in performance compared to traditional torque control methods, although chattering remained a persistent challenge [10].

Additional developments have focused on improving the robustness and accuracy of SMC methods. Zeinali and Notash (2010) combined feedback linearization with SMC, utilizing a proportional-integral-derivative (PID) controller to stabilize dynamic uncertainties in robotic systems [11]. A fuzzy logic-integrated sliding mode controller to eliminate chattering and improve the performance of a planar robot is studied by Yagiz. The effectiveness of the controller is validated through simulations, testing its robustness and noise

*Corresponding author's email: habibahmadif@shahroodut.ac.ir

resistance[12]. Piltan et al. (2011) implemented nonlinear SMC methods using field-programmable gate arrays (FPGA), demonstrating that increasing the processing frequency reduces chattering and improves system performance [13, 14]. Furthermore, Sanchez and Fierro (2003) developed a sliding mode controller for coordinating teams of non-holonomic robots, using Lyapunov's method to prove system stability and achieve trajectory tracking with acceptable error margins [15].

Despite the progress made, chattering remains a critical issue, especially in mechanical and electrical systems. To address this, several strategies have been proposed. One approach involves nonlinear gains, while another employs HOSM methods [16]. Additionally, some methods replace the discrete control signal (i.e., the signum function) with a continuous approximation function to reduce chattering [5-7, 16]. Levant (1993) demonstrated that the convergence accuracy of sliding mode control is proportional to the square of switching delay time [17], underscoring the need for minimizing chattering frequency. Bartolini et al. (1997) introduced suboptimal control designs that improve controller performance in second-order dynamic systems [18-21]. Recent advancements in SMC have introduced quantum sliding mode control for improving system performance under uncertainties. This approach uses a quantum sliding surface based on the error between the system state and the sliding mode. By combining sliding mode control with periodic projective measurements, the method reduces both reaching time and control amplitude, demonstrating its effectiveness through simulations[22].

In recent years, the use of HOSM has expanded into more complex systems, such as multi-input multi-output (MIMO) systems [18, 19, 23] Capisani et al. (2009) successfully implemented HOSM to control a COMAU SMART3-S2 robot, initially applying SMC but later shifting to HOSM to prevent damage caused by vibration in the motors and electronic components [24, 25]. Zhao et al. (2018) applied a super-twisting adaptive controller to tethered space robots, that successfully reduced chattering and improved robustness in the presence of unknown uncertainties [26]. Kali et al. (2018) integrated STA with time-delay estimation to improve robot trajectory tracking under uncertain conditions, which reduced disturbances and enhanced robustness [27]. Tayebi-Haghighi et al. (2018) demonstrated the effectiveness of HOSM as both an observer and controller for PUMA robots, significantly reducing root-mean-square error (RMSE) [28]. Van et al. also utilized HOSM to compensate for uncertainties and reduce chattering to control the PUMA 560 robot, showing finite-time convergence of the system [7]. Huang et al. introduced a robust control technique, super-twisting sliding mode control, for force actuator design in hybrid model testing of vessels in wave tanks. The proposed actuator, validated experimentally, demonstrated precise force control with minimal errors, ensuring suitability for capturing complex physical phenomena in hybrid testing scenarios[29]. An adaptive neural network integral sliding-mode controller is proposed to control a biped robot, eliminating chattering in traditional integral sliding-mode controllers. The adaptive neural network estimates disturbances, while the bat algorithm tunes the controller parameters. Lyapunov stability is proven, and simulations demonstrate the effectiveness of the controller in reducing chattering[30]. In another study, the design and analysis of a three-dimensional attitude control law for underactuated multirotor aerial vehicles is presented, addressing bounded matched disturbances and uncertainties with unknown bounds. Using a geometrically consistent Gibbs vector model, an adaptive sliding mode control strategy is developed and validated through simulations and experiments, ensuring robust performance with eventual sliding mode convergence[31].

Recent research efforts have focused on enhancing the robustness and convergence speed of sliding mode control in uncertain and dynamic environments. One such direction involves the integration of backstepping and high-order terminal sliding mode control to achieve smooth control torques and fast finite-time convergence in robotic manipulators[32]. In this context, adaptive fractional-order methods have also been proposed to reduce chattering and improve tracking accuracy without prior knowledge of system bounds, offering enhanced robustness against varying loads and disturbances[33].

Moreover, higher-order sliding mode observers have been employed to enable real-time estimation of external torques in manipulator-environment interaction scenarios. These methods, supported by Lyapunov-based Luenberger observers, demonstrate effective tracking and disturbance estimation, even under strong nonlinear friction[34]. Similarly, for systems with physical constraints such as underwater vehicles, model-free high-order sliding mode controllers have been synthesized with time-base generators to ensure finite-time convergence while significantly reducing the energy consumption of actuators[35].

Additionally, the combination of neural networks and sliding mode control has yielded promising results in power electronics. For instance, fractional-order sliding mode schemes integrated with recurrent neural networks have been shown to enhance compensation performance and robustness in active power filters [36]. Further, model-free second-order sliding mode strategies incorporating disturbance observers have been introduced to optimize torque rejection in permanent magnet synchronous motor (PMSM) systems, providing chattering-free control and finite-time stability[37].

Recent advances have further expanded HOSM applications in robotic systems. Zhang et al. (2023) developed an adaptive super-twisting algorithm that automatically adjusts control gains for manipulators with completely unknown dynamics, eliminating the need for prior knowledge of uncertainty bounds while maintaining Lyapunov stability [38]. Experimental validations on 2-DOF arms by Wang et al. (2024) demonstrated that finite-time HOSM controllers can achieve tracking accuracies below 0.1° even with payload variations up to 50%, outperforming conventional SMC in both convergence speed and steady-state error [39]. For under-actuated systems, Khan et al. (2023) introduced a novel chattering suppression technique using logarithmic barrier functions that maintains robustness while reducing control effort by 35% compared to standard HOSM approaches [40].

Given the significance of reducing chattering and improving system performance in uncertain environments, the development of new HOSM approaches is crucial. This paper presents a novel HOSM algorithm that not only mitigates chattering but also allows for the adjustment of chattering frequency through controller parameters. The stability of the proposed algorithm is rigorously proven using Lyapunov's

method, and its performance is evaluated through numerical simulations, comparing it to existing HOSM methods. As the article proceeds, Section 2 introduces the problem formulation and defines the sliding variable. The proposed high-order sliding mode controller and its stability analysis are presented in Section 3. Section 4 provides detailed numerical simulations to evaluate the performance of the controller, including comparisons with existing algorithms and application to a two-link planar robot. Finally, section 5 concludes the paper by summarizing the key findings and discussing potential future directions.

2- Problem formulation

Consider the following nonlinear dynamic equation:

$$\ddot{x} = f\left(t,x,\dot{x}\right) + g\left(t,x,\dot{x}\right)u\left(t\right) \tag{1}$$

where $x \in \mathbb{R}^n$ represents the system state and $u \in \mathbb{R}$ is the control input. The functions $f\left(t,x,\dot{x}\right)$ and $g\left(t,x,\dot{x}\right)$ are assumed to be smooth, and all states of the system in Eq. (1) are considered measurable. In this study, we introduce the sliding variable denoted by σ as a smooth function. To have a good performance for the system control, we need to define a suitable and stable sliding surface, so that this surface should converge to zero. An essential requirement for achieving a stable and robust control system is to guarantee that the variations of the sliding surface are bounded [17].

The sliding variable σ is selected so that its derivative follows the system dynamics as described in the following equation [41]:

$$\dot{\sigma} = h\left(t,x,\dot{x}\right) + g\left(t,x,\dot{x}\right)u\left(t\right) \tag{2}$$

The limitations of the controller arise from derivations of the sliding surface and system uncertainties, which are addressed through the application of the Filippov solution framework as follows [42]. The solution to this system, in the sense of Filippov, is expressed in input-output form as:

$$\begin{aligned} &\ddot{\sigma} = \phi\left(t,x,\dot{x},u\right) + g\left(t,x,\dot{x}\right)\upsilon \\ &\upsilon = \dot{u} \end{aligned} \tag{3}$$

where,

$$\begin{aligned} &\phi\left(t,x,\dot{x},u\right) = \frac{\partial}{\partial t}h\left(t,x,\dot{x}\right) + \frac{\partial}{\partial x}h\left(t,x,\dot{x}\right)\dot{x} \\ &+\frac{\partial}{\partial \dot{x}}h\left(t,x,\dot{x}\right)f\left(t,x,\dot{x}\right) \\ &+\begin{bmatrix} \frac{\partial}{\partial t}g\left(t,x,\dot{x}\right) + \frac{\partial}{\partial x}g\left(t,x,\dot{x}\right)\dot{x} \\ +\frac{\partial}{\partial \dot{x}}g\left(t,x,\dot{x}\right)\left(f\left(t,x,\dot{x}\right) + g\left(t,x,\dot{x}\right)u\left(t\right)\right) \\ +\frac{\partial}{\partial \dot{x}}h\left(t,x,\dot{x}\right)g\left(t,x,\dot{x}\right) \end{bmatrix}u\left(t\right) \end{aligned} \tag{4}$$

The following conditions are assumed for the sliding surface σ (as defined in Eq. (2)), provided that its components satisfy the following inequalities:

$$\begin{aligned} &0 < \Gamma_m \le g\left(t,x,\dot{x}\right) \le \Gamma_M \\ &\left|\sigma\right| < \sigma_0 \\ &\left|\phi\left(t,x,\dot{x},u\right)\right| < \Phi \end{aligned} \tag{5}$$

where Γ_M, Γ_m, σ_0, and Φ are positive constants. These conditions are necessary to ensure system stability on the sliding surface [17]. The limitations of the sliding surface and its applicability to different system dynamics are addressed in Eqs. (2-5). These equations define the sliding surface in the presence of system uncertainties and establish the conditions under which the proposed structure remains valid. In particular, the controller is suitable for systems whose relative degree is consistent with the order of the derivative terms defined in the sliding variable.

3- Controller

In this section, we introduce the proposed novel controller based on high-order sliding mode (HOSM) theory and analyze its stability. The design aims to reduce chattering and ensure robustness in the presence of uncertainties. The stability of the controller is proven using Lyapunov's method.

3- 1- Sliding Surface Definition

The sliding variable σ is introduced as a function of the system state and its derivatives. For a second-order dynamic system, the sliding surface is defined as:

$$\sigma = \dot{x} + \lambda x \tag{6}$$

where λ is a positive constant that defines the sliding dynamics. The sliding surface is designed to constrain system behavior, ensuring robust performance under uncertainties. When the system reaches this surface, it is forced to remain stable on it.

3- 2- Controller Design

The following second-order sliding mode control law is proposed for systems where $\left|\sigma\right| \le \sigma_0$:

$$\begin{aligned} &\ddot{\sigma} + K_1\left(\frac{\pi}{2\sigma_0}\right)\dot{\sigma}\cos\left(\frac{\sigma\pi}{2\sigma_0}\right) \\ &+K_2\,\mathrm{sgn}\left(\sigma\right) = 0 \,\text{for}\, \left|\sigma\right| \le \sigma_0 \end{aligned} \tag{7}$$

where K_1, K_2, and σ_0 are control parameters that ensure system stability, and the signum function $\mathrm{sgn}\left(\sigma\right)$ drives the system towards the sliding surface. This equation is designed to minimize the chattering effect while maintaining robust control.

3- 3- Controller Implementation

By substituting the system of Eq. (1) into the control law,

the control input $u(t)$ is derived as:

$$u = u_{eq} - \frac{1}{\hat{g}}\left[K_1 \sin\left(\frac{\sigma\pi}{2\sigma_0}\right) + K_2 \int \mathrm{sgn}(\sigma)dt\right], \quad |\sigma| \le \sigma_0 \tag{8}$$

where $u_{eq} = -\frac{1}{\hat{g}}\left(\hat{f} + \lambda\dot{x}\right)$ is the equivalent control term stabilizing the nominal system. This equation ensures smooth control actions with reduced chattering.

3- 4- Stability Analysis

The stability of the proposed sliding mode control method consists of two parts. First, it is essential to prove that under bounded uncertainty, all system states will converge to zero while remaining on the sliding surface [6]. Second, the stability of the dynamic equation of the sliding variable must be demonstrated, ensuring convergence to the sliding surface.

To establish the stability of the controller, Lyapunov's method is employed. The sliding mode dynamics are rewritten in the state-space form as:

$$\begin{cases} \dot{\sigma}_1 = -K_1 \sin\left(\frac{\sigma_1\pi}{2\sigma_0}\right) + \sigma_2 \\ \dot{\sigma}_2 = -K_2 \,\mathrm{sgn}(\sigma_1) \end{cases} \tag{9}$$

$$\sigma_1 = \sigma$$
$$\sigma_2 = -K_2 \int \mathrm{sgn}(\sigma)dt$$

A Lyapunov candidate function is defined as:

$$V = \frac{1}{2K_2}\sigma_2^2 + |\sigma_1| \tag{10}$$

Taking the derivative of the Lyapunov function yields:

$$\dot{V} = -K_1 \sin\left(\frac{\sigma_1\pi}{2\sigma_0}\right)\mathrm{sgn}(\sigma_1), \quad \sigma_0 > 0, |\sigma_1| \le \sigma_0 \Rightarrow \dot{V} \le 0 \tag{11}$$

Since $\dot{V} \le 0$, it follows from Lyapunov's theorem that the proposed controller is stable, ensuring convergence of the system to the sliding surface. This guarantees that the system states remain bounded and tend to zero over time.

4- Numerical simulation

4- 1- Simple System Comparison

To evaluate the performance of the proposed control algorithm, numerical simulations were conducted using a system where $\ddot{x} = u$. The sliding surface for all simulations was defined as $\sigma = \dot{x} + \lambda x$, with $\lambda = 5$ and the equivalent control input $u_{eq} = -\lambda\dot{x}$. The parameters for the proposed controller were set as $K_1 = 9$, $K_2 = 7$ and $\sigma_0 = 0.1$. The simulations were performed with a sampling time of one millisecond to ensure sufficient precision.

Fig. 1 depicts the phase plane of the sliding states under the proposed controller. As observed, the sliding variable remains close to the sliding surface, corroborating the stability proof established using Lyapunov's method. This behavior confirms that the proposed controller ensures the system states converge to the sliding surface with minimal deviation.

To further investigate the effects of the sliding surface parameter σ_0, its value was varied, and the system's response was plotted in Fig. 2. It was found that decreasing σ_0 resulted in the sliding dynamics reaching the sliding

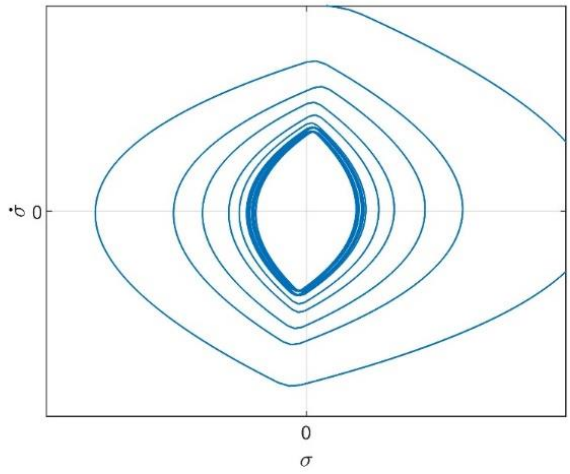

Fig. 1. Phase plane of the sliding states for the proposed controller

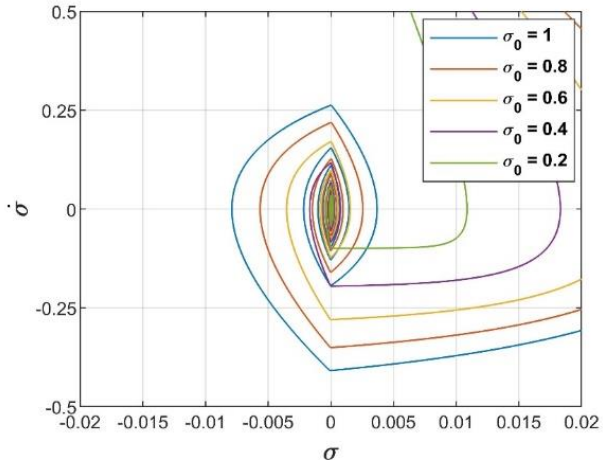

Fig. 2. Effect of varying σ_0 on the sliding dynamics

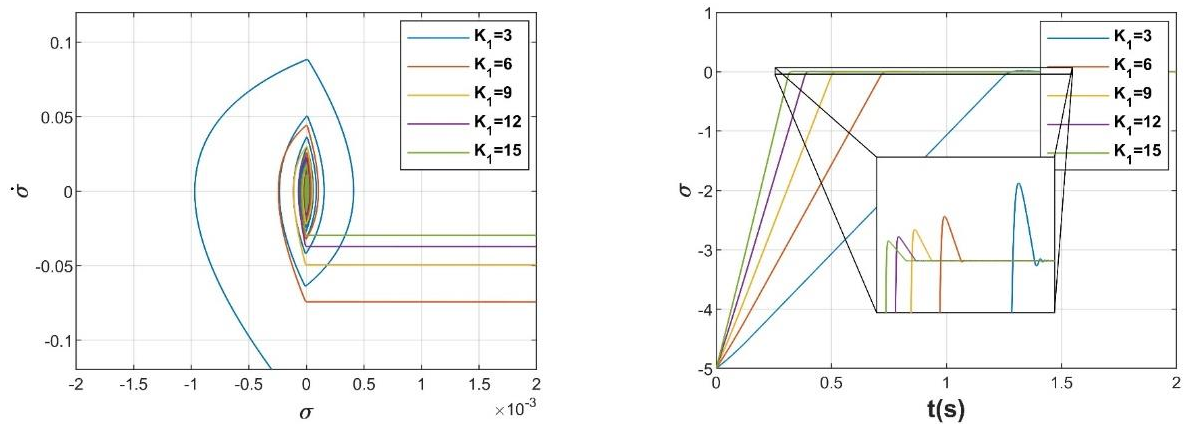

(a) (b)

Fig. 3. Effect of varying K_1 on system response

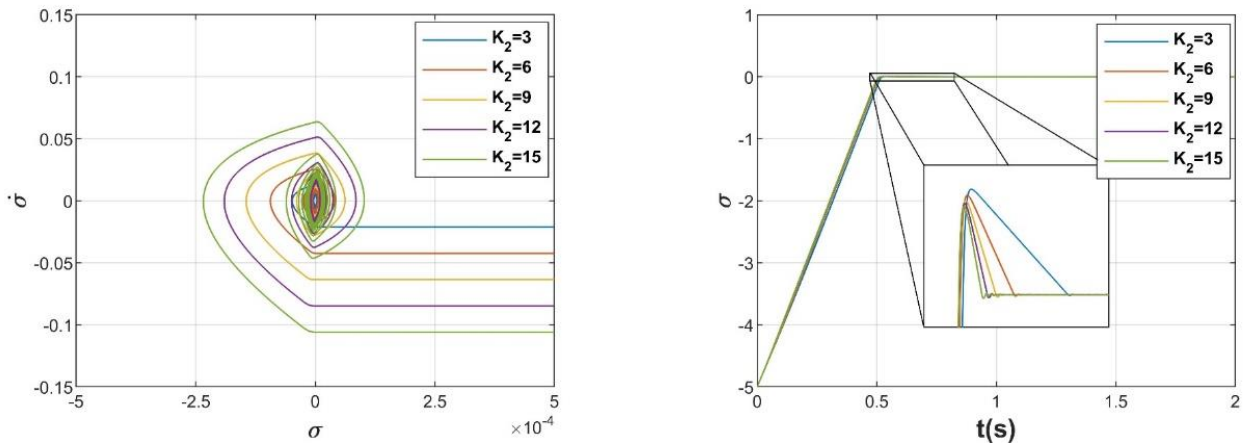

(a) (b)

Fig. 4. Effect of varying K_2 on sliding dynamics

surface more rapidly. However, this led to an increase in the frequency of chattering, as evident in the $\dot{\sigma}-\sigma$ phase diagram. Conversely, increasing σ_0 reduced the chattering frequency but also increased the amplitude, demonstrating the trade-off between chattering frequency and amplitude.

Fig. 3 illustrates the impact of changing the coefficient K_1 on system performance. As expected, increasing K_1 enhanced the speed at which the system reached the sliding surface, particularly when the system was far from the surface. However, the effect of K_1 on the system response near the sliding surface is insignificant. Fig. 3(a) and Fig. 3(b) show that reducing K_1 increases the amplitude of chattering, since the overall response of the system diminishes. Additionally, increasing the system's response speed requires a corresponding increase in the control input, indicating that the controller's input must be appropriately tuned for optimal performance.

Next, we analyzed the effects of varying the parameter K_2, which primarily influences the system's behavior near the sliding surface. As shown in Fig. 4, increasing K_2 resulted in faster convergence to the sliding surface, as well as an increase in the frequency of chattering. However, this also caused a slight increase in the amplitude of chattering near the surface, as illustrated in Fig. 4(a). The trade-off between chattering frequency and convergence speed becomes evident when adjusting K_2, highlighting the need for careful tuning to balance system stability and response characteristics.

Fig. 2 demonstrates the impact of varying the parameter σ_0 on the sliding dynamics, revealing how the approach to the sliding surface is affected. Fig. 3 illustrates how changes

in the gain parameter K_1 influence the overall system response, including convergence rate and control smoothness. Fig. 4 highlights the sensitivity of the sliding dynamics to variations in K_2, offering insights into the trade-off between speed and stability. These results confirm that while the proposed controller shows sensitivity to tuning parameters, it maintains robust performance across a practical tuning range. This tunability enhances its adaptability to various system requirements and operating conditions, making it suitable for real-world applications.

Based on the conducted simulations, it can be concluded that the slope of the cosine derivative at zero is regulated by the parameter σ_0. This slope, in contrast to the square root function used in the super-twisting controller, is tunable via σ_0. In practice, the key innovation of this study, namely the tuning of chattering frequency, is directly achieved through this parameter. While the parameter K_1 in the controller can also influence both error and frequency, σ_0 alone enables a trade-off between these two aspects. This property significantly enhances the practical applicability and tunability of the proposed controller. While the trade-off between chattering amplitude and frequency is adjustable within the proposed controller, the control performance can be tailored to meet system requirements and operational conditions. Uncertainties and external disturbances introduce energy fluctuations into the system, which, based on Lyapunov theory, must be compensated by the controller. Given that the proposed controller utilizes sinusoidal and cosinusoidal functions, the injected energy manifests in terms of frequency and amplitude. Consequently, the trade-off between these two parameters behaves analogously to that of the derivative of a cosine function, allowing precise tuning of control characteristics. Accordingly, increasing the value of σ_0 leads to a decrease in chattering frequency; however, this comes at the cost of increased chattering amplitude and higher root mean square error. Conversely, decreasing σ_0 reduces the amplitude and RMS error while raising the chattering frequency. Therefore, to tune the chattering characteristics, the parameter σ_0 is initially set to a relatively high value (e.g., 1). Then, σ_0 is gradually decreased in a stepwise manner, during which the chattering amplitude increases while the tracking error decreases. This process is repeated until the chattering remains within a tolerable level and the error falls below the desired threshold.

4- 2- Comparison with TA and STA

To further evaluate the performance of the proposed algorithm, a comparative study was conducted between the novel controller, the Twisting Algorithm, and the Super-Twisting Algorithm. The sliding surface was defined similarly for all three controllers to ensure consistency in the comparison. The parameters for each controller were tuned to provide the best performance in terms of system input.

In order to facilitate a comparative analysis of the controllers and investigate the impact of system uncertainties, a representative dynamic model is formulated as Eq. (12).

$$\ddot{x} = (1+\delta\varphi_1)u(t) + \delta\varphi_2 \tag{12}$$

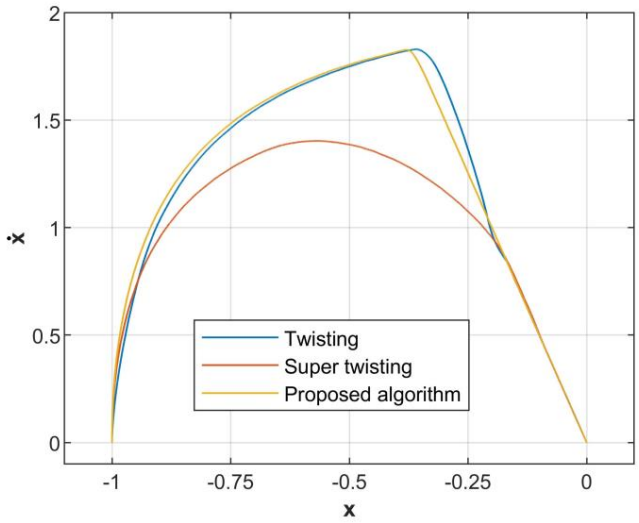

Fig. 5. Phase plane comparison of sliding states for TA, STA, and proposed controller

where $\delta\varphi_1$ and $\delta\varphi_2$ represent the uncertainties in the form of random functions as follows:

$$\delta\varphi_1 = \text{rand}[-0.2, 0.2]$$
$$\delta\varphi_2 = \text{rand}[-1, 1]$$

It should be noted that a sample time of one millisecond has been employed for the numerical simulations. This reflects our intention to align the control structure with real-time constraints even in the simulation phase, ensuring feasibility for future implementation.

Fig. 5 presents the phase plane trajectories for all three controllers. The results show that the novel controller reaches the sliding surface more quickly than both of TA and STA and remains closer to the surface throughout the simulation. Additionally, the STA exhibited a smaller amplitude of chattering compared to the other controllers, as seen in the detailed phase diagrams.

Due to the nonlinear nature of the proposed controller, the convergence function does not admit a simple analytical form. Instead, the convergence behavior is illustrated through phase-plane representations. As shown in Fig. 1 and Fig. 5, the system trajectories converge to the sliding surface and exhibit finite-time stabilization characteristics.

The chattering characteristics were further analyzed by comparing the control inputs of the three algorithms, as shown in Fig. 6. The amplitude and frequency of the control input for TA were notably higher than those of the proposed algorithm. While the STA showed the smallest chattering amplitude, the proposed controller significantly reduced the chattering frequency compared to both TA and STA, offering a balanced performance in terms of stability and control effort.

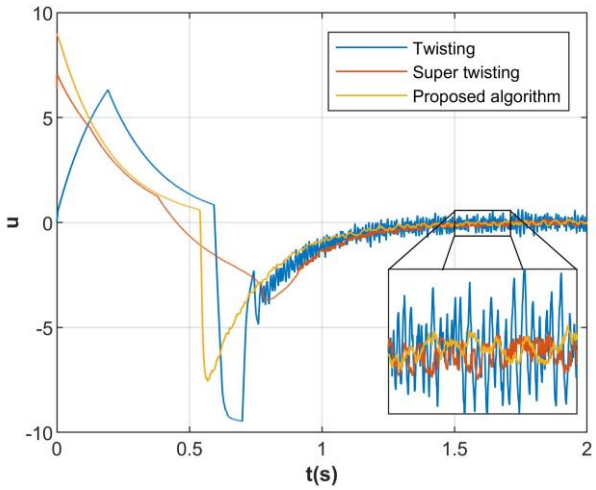

Fig. 6. Comparison of system input for TA, STA, and proposed controller

4- 3- Two-Link Planar Robot Simulation

To further validate the performance of the proposed controller, a simulation was conducted on a two-link (2R) planar robot manipulator. The dynamics of the robot were described by the following equation:

$$\mathbf{M}(\mathbf{q})\ddot{\mathbf{q}}+\mathbf{C}(\mathbf{q},\dot{\mathbf{q}})+\mathbf{G}(\mathbf{q})=\boldsymbol{\tau} \tag{13}$$

where $\mathbf{q}=[q_1,q_2]^T$ represents the joint positions, $\mathbf{M}(\mathbf{q})$ is the inertia matrix, $\mathbf{C}(\mathbf{q},\dot{\mathbf{q}})$ is the Coriolis matrix, and $\mathbf{G}(\mathbf{q})$ is the gravitational term[12]. The sliding surface for the two-link robot was defined as $\sigma=\dot{q}+\lambda q$, consistent with the formulation used in the previous simulations.

The initial conditions for the robot were set as:

$$q_1(0)=\frac{\pi}{6},\ \dot{q}_1(0)=0$$
$$q_2(0)=\frac{\pi}{6},\ \dot{q}_2(0)=0$$

And desired values were set as:

$$q_{1d}=0,\ \dot{q}_{1d}=0$$
$$q_{2d}=0,\ \dot{q}_{2d}=0$$

The simulation compared the proposed algorithm with the TA and STA. Table 1 summarizes the results in terms of average error, root mean square error (RMSE), chattering frequency, and steady-state error for both links of the robot.

The results indicate that the proposed controller achieved a significant reduction in chattering frequency compared to both of TA and STA, while maintaining similar performance in terms of tracking accuracy and RMSE. Additionally, the steady-state error was lower for both links of the robot when using the proposed algorithm, highlighting its effectiveness in achieving precise control with reduced chattering.

The implementation of the proposed controller poses several practical challenges, including sampling rate, sensor noise, actuator limitations, and external disturbances. Increasing the sampling and processing rates can effectively reduce both chattering frequency and tracking error. To mitigate sensor noise, low-pass filters can be applied; however, this creates a delay in the controller response, potentially degrading system performance. Nonetheless, by properly designing the filter characteristics, the adverse effects on control dynamics can be minimized. Another critical factor is actuator capacity. The actuator must not only generate the required control input magnitude but also be capable of tracking its rapid variations. To enhance actuator and overall control system performance, the actuator dynamics can be incorporated into the controller design, or a dedicated inner-loop controller can be employed. Overall, the control constraints are formulated in Eq. (5).

Table 1. Comparisons between TA, STA, and the new algorithm for planar robot

	Average error (m)		*RMSE*		*Chattering frequency (Hz)*		*steady-state error (×10⁻⁵m)*	
	q_1	q_2	q_1	q_2	q_1	q_2	q_1	q_2
TA	0.0566	0.0574	12.67	12.84	130.75	130.97	3.00	2.89
STA	0.0561	0.0536	12.58	12.81	117.00	100.49	2.78	3.44
Proposed	0.0556	0.0534	12.41	11.95	81.07	54.70	2.43	2.06

5- Conclusions

In this study, a novel control algorithm based on high-order sliding mode (HOSM) theory was proposed. The controller was designed to address key challenges in nonlinear systems, particularly reducing the chattering phenomenon while ensuring robust performance in the presence of uncertainties and disturbances. The stability of the proposed controller was rigorously proven using Lyapunov's method, ensuring that the system states converge to the sliding surface and remain stable.

- The key contributions and findings of this study can be summarized as follows:
- The novel algorithm provides a stable and robust control framework, with the ability to adjust the frequency and amplitude of chattering through appropriate tuning of control parameters.
- Increasing the value of σ_0 results in a decrease in chattering frequency, while decreasing it leads to an increase in frequency. This flexibility allows the controller to adapt to different system requirements.
- The parameter K_1 directly influences the speed at which the system reaches the sliding surface, with higher values resulting in faster convergence.
- In the presence of uncertainties, the proposed controller demonstrated superior performance compared to the TA and STA, significantly reducing the chattering frequency while maintaining robust control.

Through extensive numerical simulations, including tests on a two-link planar robot, the proposed controller was shown to outperform existing HOSM algorithms in terms of both tracking accuracy and chattering reduction. These results suggest that the proposed algorithm is highly suitable for controlling nonlinear systems with significant uncertainties, such as robotic manipulators.

In future work, the applicability of this controller could be extended to multi-input multi-output (MIMO) systems and more complex robotic architectures, where further tuning and adjustments may yield even greater improvements in control performance.

References

[1] V. Utkin, Variable structure systems with sliding modes, IEEE Transactions on Automatic control, 22(2) (1977) 212-222.

[2] L. Fridman, J. Moreno, R. Iriarte, Sliding modes after the first decade of the 21st century, Lecture notes in control and information sciences, 412 (2011) 113-149.

[3] E. Bailey, A. Arapostathis, Simple sliding mode control scheme applied to robot manipulators, International Journal of Control, 45(4) (1987) 1197-1209.

[4] H. Hashimoto, K. Maruyama, F. Harashima, A microprocessor-based robot manipulator control with sliding mode, IEEE Transactions on Industrial Electronics, (1) (1987) 11-18.

[5] S. Emelyanov, S. Korovin, L. Levantovskiy, A drift algorithm in control of uncertain processes, PROB. CONTROL INFO. THEORY., 15(6) (1986) 425-438.

[6] S. Emel'Yanov, S. Korovin, A. Levant, High-order sliding modes in control systems, Computational mathematics and modeling, 7(3) (1996) 294-318.

[7] M. Van, H.-J. Kang, K.-S. Shin, Novel quasi-continuous super-twisting high-order sliding mode controllers for output feedback tracking control of robot manipulators, Proceedings of the Institution of Mechanical Engineers, Part C: Journal of Mechanical Engineering Science, 228(17) (2014) 3240-3257.

[8] K.S. Yeung, Y.-P. Chen, Regulation of a one-link flexible robot arm using sliding-mode technique, International Journal of Control, 49(6) (1989) 1965-1978.

[9] C.Y. Su, T.P. Leung, A sliding mode controller with bound estimation for robot manipulators, IEEE Transactions on Robotics and Automation, 9(2) (1993) 208-214.

[10] S. Tzafestas, M. Raibert, C. Tzafestas, Robust sliding-mode control applied to a 5-link biped robot, Journal of Intelligent and Robotic Systems, 15(1) (1996) 67-133.

[11] M. Zeinali, L. Notash, Adaptive sliding mode control with uncertainty estimator for robot manipulators, Mechanism and Machine Theory, 45(1) (2010) 80-90.

[12] N. Yagiz, Y. Hacioglu, Fuzzy sliding modes with moving surface for the robust control of a planar robot, Journal of Vibration and Control, 11(7) (2005) 903-922.

[13] F. Piltan, S. Emamzadeh, Z. Hivand, F. Shahriyari, M. Mirazaei, PUMA-560 robot manipulator position sliding mode control methods using MATLAB/SIMULINK and their integration into graduate/undergraduate nonlinear control, robotics and MATLAB courses, International Journal of Robotics and Automation, 3(3) (2012) 106-150.

[14] F. Piltan, A. Gavahian, N. Sulaiman, M.H. Marhaban, R. Ramli, Novel Sliding Mode Controller for robot manipulator using FPGA, Journal of Advanced Science & Engineering Research, 1(1) (2011) 1-22.

[15] J. Sanchez, R. Fierro, Sliding mode control for robot formations, in: Proceedings of the 2003 IEEE International Symposium on Intelligent Control, IEEE, 2003, pp. 438-443.

[16] M.K. Khan, Design and application of second-order sliding mode control algorithms, (2003).

[17] [17] A. Levant, Sliding order and sliding accuracy in sliding mode control, International Journal of Control, 58(6) (1993) 1247-1263.

[18] G. Bartolini, A robust control design for a class of uncertain non-linear systems featuring a second-order sliding mode, International Journal of Control, 72(4) (1999) 321-331.

[19] G. Bartolini, A. Ferrara, E. Punta, Multi-input second-order sliding-mode hybrid control of constrained manipulators, Dynamics and Control, 10 (2000) 277-296.

[20] G. Bartolini, A. Ferrara, E. Usai, Applications of a sub-optimal discontinuous control algorithm for uncertain second order systems, International Journal of Robust and Nonlinear Control: IFAC-Affiliated Journal, 7(4) (1997) 299-319.

[21] G. Bartolini, A. Ferrara, E. Usai, Chattering avoidance by second-order sliding mode control, IEEE Transactions on Automatic Control, 43(2) (1998) 241-246.

[22] S. Chegini, M. Yarahmadi, Quantum sliding mode control via error sliding surface, Journal of Vibration and Control, 24(22) (2018) 5345-5352.

[23] A. Ferrara, On multi-input backstepping design with second order sliding modes for a class of uncertain nonlinear systems, International Journal of Control, 71(5) (1998) 767-788.

[24] L.M. Capisani, A. Ferrara, L. Magnani, Second order sliding mode motion control of rigid robot manipulators, in, IEEE, pp. 3691-3696.

[25] L.M. Capisani, A. Ferrara, L. Magnani, Design and experimental validation of a second-order sliding-mode motion controller for robot manipulators, International Journal of Control, 82(2) (2009) 365-377.

[26] Y. Zhao, P. Huang, F. Zhang, Dynamic modeling and super-twisting sliding mode control for tethered space robot, Acta Astronautica, 143 (2018) 310-321.

[27] Y. Kali, M. Saad, K. Benjelloun, C. Khairallah, Super-twisting algorithm with time delay estimation for uncertain robot manipulators, Nonlinear Dynamics, 93(2) (2018) 557-569.

[28] S. Tayebi-Haghighi, F. Piltan, J.-M. Kim, Robust composite high-order super-twisting sliding mode control of robot manipulators, Robotics, 7(1) (2018) 13.

[29] A.S. Huang, E.A. Tannuri, P.C. de Mello, Development of a force actuator for hybrid model tests using super-twisting sliding mode control, Journal of the Brazilian Society of Mechanical Sciences and Engineering, 43 (2021) 1-12.

[30] M. Rahmani, H. Komijani, M.H. Rahman, New sliding mode control of 2-DOF robot manipulator based on extended grey wolf optimizer, International Journal of Control, Automation and Systems, (2020) 1-9.

[31] D.A. Santos, J.F. Trentin, J.A. Ricardo Jr, L.G.P. Roéfero, T.R. Oliveira, Adaptive sliding mode attitude control for multirotor aerial vehicles with experimental evaluation, Journal of the Brazilian Society of Mechanical Sciences and Engineering, 46(4) (2024) 194.

[32] T.N. Truong, A.T. Vo, H.-J. Kang, A backstepping global fast terminal sliding mode control for trajectory tracking control of industrial robotic manipulators, IEEE Access, 9 (2021) 31921-31931.

[33] S. Ahmed, H. Wang, Y. Tian, Adaptive fractional high-order terminal sliding mode control for nonlinear robotic manipulator under alternating loads, Asian Journal of Control, 23(4) (2021) 1900-1910.

[34] S.K. Kommuri, S. Han, S. Lee, External torque estimation using higher order sliding-mode observer for robot manipulators, IEEE/ASME Transactions on Mechatronics, 27(1) (2021) 513-523.

[35] J. Gonzalez-Garcia, N.A. Narcizo-Nuci, L.G. Garcia-Valdovinos, T. Salgado-Jimenez, A. Gómez-Espinosa, E. Cuan-Urquizo, J.A.E. Cabello, Model-free high order sliding mode control with finite-time tracking for unmanned underwater vehicles, Applied Sciences, 11(4) (2021) 1836.

[36] J. Fei, H. Wang, Y. Fang, Novel neural network fractional-order sliding-mode control with application to active power filter, IEEE transactions on systems, man, and cybernetics: systems, 52(6) (2021) 3508-3518.

[37] S. Ding, Q. Hou, H. Wang, Disturbance-observer-based second-order sliding mode controller for speed control of PMSM drives, IEEE Transactions on Energy Conversion, 38(1) (2022) 100-110.

[38] J. Zhang, Y. Li, K. Xu, Adaptive Super-Twisting Sliding Mode Control for Robotic Manipulators with Unknown Dynamics, IEEE Transactions on Industrial Electronics, 70(5) (2023) 4125-4136.

[39] M. Wang, S. Chen, L. Liu, Finite-Time High-Order Sliding Mode Control for 2-DOF Robot Arms: Experimental Validation, Robotics and Autonomous Systems, 173 (2024) 104567.

[40] A. Khan, R. Patel, T. Sharma, Chattering-Free Sliding Mode Control for Underactuated Robots Using Barrier Functions, International Journal of Robust and Nonlinear Control, 33(15) (2023) 8912-8930.

[41] A. Levant, L. Alelishvili, Integral high-order sliding modes, IEEE Transactions on Automatic control, 52(7) (2007) 1278-1282.

[42] A.F. Filippov, Differential equations with discontinuous righthand sides: control systems, Springer Science & Business Media, 2013.

HOW TO CITE THIS ARTICLE

M. Abdolmohammadi, H. Ahmadi, Presenting of a novel high-order sliding mode control based on Lyapunov theory, AUT J. Mech Eng., 9(4) (2025) 403-412.

DOI: 10.22060/ajme.2025.23879.6163